Identification of Schizophrenia from fMRI and MEG Signals Through a 3D CNN-Based Deep Learning Model

Mehzabeen S.M.[1]
Assistant professor
Department of electronics and communication engineering,
Sri Venkateswara college of engineering Chennai, India
mehzabeen@svce.ac.in

Akeel Ahamed R S [2]
Department of Computer Science and engineering,
Sri Venkateswara college of engineering,
Chennai, India
2022cs0365@svce.ac.in

Cletus Rajkumar[3]
Department of Computer Science and engineering,
Sri Venkateswara college of engineering,
Chennai, India
2022cs0113@svce.ac.in

***Abstract*:**

According to World Health Organization (WHO), schizophrenia affects about 1 in 300 people (0.32%) worldwide, and 1 in 222 adults (0.45%).The disorder typically emerges in late adolescence or early adulthood, with men often showing symptoms earlier (late teens to early 20s) than women (early to late 20s).Individuals with schizophrenia are at a 2 to 3 times higher risk of premature death, primarily due to preventable physical health conditions.It contributes to a significant global disease burden, with a large portion of affected individuals facing social stigma, discrimination, and reduced access to healthcare and employment.Despite being treatable, over 50% of people with schizophrenia do not receive adequate mental health care, especially in low- and middle-income countries. It is a chronic illness that can severely impact an individual's cognitive, emotional, and behavioural functions. Early detection and diagnosis of schizophrenia are critical for effective treatment, but it can be challenging to identify it in its early stages due to the complexity of its symptoms.

Functional magnetic resonance imaging (fMRI) has been used to identify functional changes in the brain of individuals with schizophrenia. However, manual analysis of these images can be time-consuming and prone to human error. Convolutional neural networks (CNNs) have recently shown great potential in the automatic detection and classification of various medical conditions, including neurological disorders. Therefore, the development of an automated CNN-based method to diagnose schizophrenia using functional MRI could potentially improve the accuracy and efficiency of schizophrenia diagnosis.

Magnetoencephalography (MEG) is a non-invasive neuroimaging technique that detects brain activity by measuring the tiny magnetic fields generated by neural activity within the brain. In this review, we will discuss the recent advancements in CNN-based methods for identifying schizophrenia using functional MRI. Firstly, we will provide an overview of the structural changes in the brain of individuals with schizophrenia that can be detected using functional MRI. Next, we will describe the basic concepts of CNNs and the training process for medical image analysis. We will then discuss the different CNN architectures that have been used for the identification of schizophrenia using functional MRI, including the 2D and 3D CNNs.In conclusion, CNN-based methods have shown great potential in identifying schizophrenia using functional MRI, with high accuracy rates reported in several studies. However, further research is needed to address the challenges and limitations of these methods.

Schizophrenia is a chronic and severe mental health disorder that significantly impacts an individual's thoughts, emotions, and behavior. It is a complex condition characterized by a diverse range of symptoms that can vary widely in both severity and frequency among individuals. Globally, it is estimated to affect about 1% of the population, accounting for nearly 24 million people worldwide.The exact causes of schizophrenia are not fully understood, but research suggests that a combination of genetic, environmental, and developmental factors may contribute to the development of the disorder. Abnormalities in brain structure and function, particularly in the prefrontal cortex and other regions involved in the regulation of cognition and emotion, are also thought to play a critical role. The symptoms of Schizophrenia commonly include hallucinations (perceiving sights, sounds, sensations, or

smells that are not real), delusions (strongly held false beliefs not grounded in reality), disorganized thinking and speech, social withdrawal, diminished emotional expression, and a flat or blunted affect.

Both Functional magnetic resonance imaging (fMRI) and Magnetoencephalography (MEG) provide complementary insights into brain function, yet they also produce vast amounts of complex data that are challenging to analyze without losing critical information. For instance, the blood oxygenation-level dependent (BOLD) signal captured by fMRI enables clear visualization of the spatial extent and distribution of brain activation. However, it reflects an indirect and slowly evolving physiological response, limiting its ability to track rapid neural events. In contrast, MEG measures neural oscillatory activity—rhythmic electrical patterns in neuronal assemblies—within the 1–900 Hz frequency range, offering high temporal resolution. Since fMRI cannot accurately capture such fast electrical impulses, integrating both techniques within the same participant sample allows researchers to leverage the strengths of each modality, enabling meaningful comparisons and a more comprehensive understanding of brain activity.

I. DATA ACQUISITION AND PROCESSING

A. *Data set:*

The features presented in this work are the outcome of recent state-of-the-art advancements in neuro-imaging and MRI data processing. These features are obtained using MEG and functional MRI. This study discusses how to select elements that improve diagnosis and how to best combine this kind of multimodal information.

The fMRI dataset contains labels for the dataset. The labels are indicated in the "Class" column. 0 = 'Healthy Control', 1 = 'Schizophrenic Patient'. The dataset contains FNC features. These are correlation values. They describe the connection level between pairs of brain maps over time.In addition to it , the dataset contains SBM features. These are standardized weights. They describe the expression level of ICA brain maps derived from grey-matter concentration.

Id	FNC1	FNC2	FNC3	FNC4	FNC5	FNC6
120873	0.34312	0.045761	-0.13112	0.15034	0.18082	0.28916
135376	0.2879	0.10257	-0.32343	-0.22776	0.12328	0.36702
139149	0.24585	0.21662	-0.12468	-0.3538	0.1615	-0.00203
146791	0.4209	0.33138	0.24453	0.17167	0.59223	0.43105
153870	-0.14621	-0.46863	-0.5288	-0.50381	-0.51052	-0.02911
167403	0.55836	0.35646	0.35729	0.28911	0.2762	0.44263
179564	0.113	-0.43457	-0.71167	-0.70187	0.12693	-0.39747
179614	0.40232	0.06261	0.36089	0.18163	0.41605	-0.26195

Figure 1. represents tabulated values of FNC features of Healthy controls and Schizophrenic patients

.

Id	SBM_map	SBM_map	SBM_map	SBM_map	SBM_map	SBM_map
120873	0.725065	-0.63925	0.353069	-0.98171	-1.41997	-0.44132
135376	-1.32886	0.50297	0.013232	1.128496	-0.07074	0.398476
139149	0.732268	-1.24155	0.654942	-0.28922	0.158316	0.029165
146791	-0.34392	-1.05252	-1.15052	0.765989	0.923129	0.674052
153870	-0.20869	-0.5627	-0.36216	1.025571	0.15169	-0.13041
167403	-0.00953	-0.37117	-0.34809	0.994007	1.113957	-1.84722
179564	1.179198	-0.34965	0.659046	1.673886	1.125081	-0.42705
179614	1.390514	1.356896	0.444022	0.134587	0.51929	-0.85909

Figure 2. Represents tabulated values of SBM features of Healthy controls and Schizophrenic patients

B. *Data Pre-processing*

fMRI:

An fMRI volume comprises fluctuations that we are not interested in, such as head movements, random drifts, breathing, and heartbeats, in addition to the signal that we are interested in—changes in oxygenated blood. Since we want to distinguish these additional fluctuations from the signal that is of interest, we refer to them as noise. Some of them can be decreased or eliminated by preprocessing, while others can be modelled out of the data and regressed out (this is covered in the chapter on modelling fitting).
Statistical parametric mapping is an image processing method that evaluates the significance of cerebral hemodynamic alterations on a voxel-by-voxel basis using automated statistical comparison to a sample of healthy participants.

To begin processing,we will start with Realignment and Slice-Timing Correction, which fix misalignments and timing issues in the functional images. In order to boost signal and eliminate noise, the pictures are then Smoothed .Then we move onto Coregistration and Normalisation, which align the functional and structural pictures and place them both in a standardized space .Finally, Smoothing is applied to the images to boost signal and remove noise.

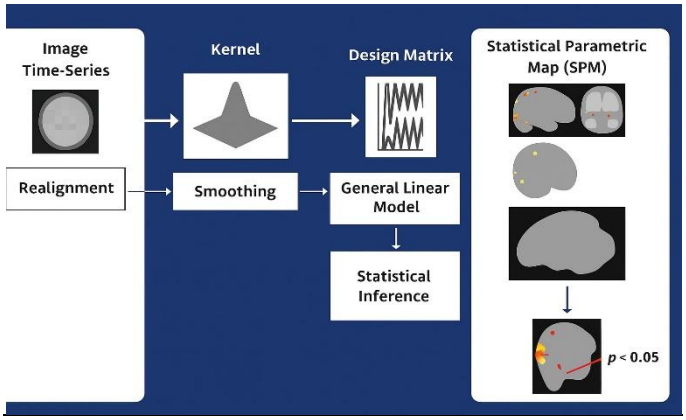

Figure 3. Represents the step by step process of Statistical parametric mapping

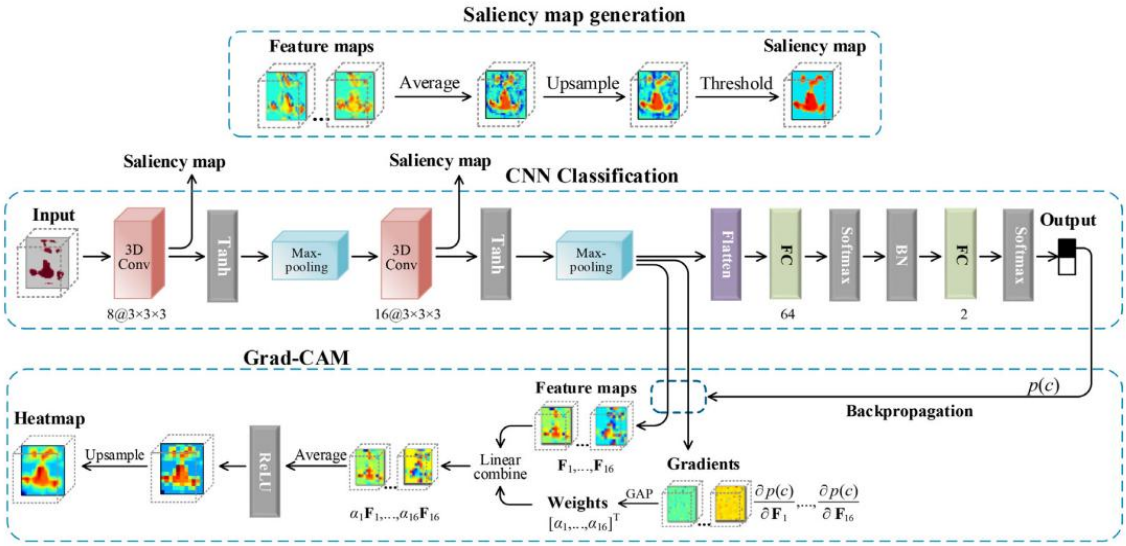

Figure 4 .The suggested interpretable SSPNet and CNN model. The output gives the odds that the input sample comes from a patient with schizophrenia or a healthy control. The input contains a 3D SSP map

MEG:

Maxfilter software was used to perform artefact removal, head movement correction, and downsampling to 250 Hz with 123 basis vectors, a spatiotemporal buffer of 10 s, and a correlation limit of r=0.95. Signal-space projection (SSP) method was used to eliminate cardiac and blink artefacts. In order to focus on four frequency ranges of interest, the data were bandpass filtered: delta (1-4 Hz), theta (5-9 Hz), alpha (10-15 Hz), and beta (16-29 Hz).

Using all of the recorded data, covariance matrices were created independently for each subject and frequency band. The minimal singular value of the unregularized matrix was multiplied by 4 to regularise covariance matrices. In other words, we added a constant to the diagonal of the matrix after estimating the covariance matrix. The constant added was four times the unregularized covariance matrix's minimal singular value. A standard 6-mm3 grid spanning the brain picture was used to place the voxels. A nonlinear search for the highest projected signal-to-noise ratio served as the foundation for source direction at each voxel. The solution was based on a single-shell boundary element model and a dipole model. For every subject and frequency range, a single beamformer projection was carried out. Source-space signals were normalised by an estimate of projected noise after beamformer projection and transformed to standard (MNI) space using FLIRT in FSL. The analytic signal was derived by applying a Hilbert transform to the time course at each voxel time. This analytical signal's absolute value was calculated to produce the Hilbert envelope, which is an amplitude envelope of oscillatory power. Each voxel's Hilbert envelope was downsampled to an effective sampling rate of 1 Hz. For ease of comparison with fMRI data, source space envelope data were spatially smoothed (6 mm3 at full-width half-maximum), and the voxel size was resampled to 333 mm.Beamformer failure can result from significant and persistent correlations between brain regions, however this requires correlations to last for 30–40% of the period under study, which is improbable with resting data.

II. Model Generation

The issue of categorizing all three types of features namely, intensity with minimal preprocessing, grey matter density, and local volume changes was resolved using 3D convolutional neural networks. No feature selection technique was used in this experiment because the convolutional neural network can extract significant features on its own.

The convolutional neural networks (CNNs) have demonstrated promising results in the classification of people suffering from mental diseases like schizophrenia using fMRI data collected during the resting state.

Despite the fact that extra phase data provides high-level noise it has the potential to be helpful information in the context of classification . As a result, we suggest that the CNN input be made up of spatial source phase (SSP) maps produced from complex-valued fMRI data. In addition to being less noisy than magnitude maps, SSP maps are also more sensitive to changes in spatial activation brought on by mental illnesses. To thoroughly investigate the 3D structure and voxel-level interactions from the SSP maps, we construct a 3D-CNN framework with two convolutional layers (called SSPNet). The well-trained SSPNet incorporates two interpretability modules—saliency map generation and gradient-weighted class activation mapping (Grad-CAM)—to give additional information that is useful for comprehending the output.

The proposed SSPNet significantly increased accuracy and AUC compared to CNN when magnitude maps were extracted

from either magnitude-only or complex-valued fMRI data (by 23.4 and 23.6% for DMN and 10.6 and 5.8% for DMN, respectively). This was demonstrated in experimental results from classifying schizophrenia patients (SZs) and healthy controls (HCs).

SSPNet captured more pronounced HC-SZ disparities in saliency maps and Grad-CAM located all contributing brain areas with contrasting intensities for HCs and SZs within SSP maps. These findings indicate SSPNet's potential as a sensitive tool that might be helpful in the creation of brain-based biomarkers for mental illnesses.

C. *CNN Model*

We build a 3D-CNN model with two convolutional layers, two maxpooling layers, two fully connected layers with 64 nodes each and two nodes each, and a layer with two nodes for the output.

The convolutional layers' kernel sizes are 3*3*3, their respective convolutional kernel counts are 8 and 16, and the pooling layer's filter size is 2* 2* 2. The convolutional layers' activation function is set to Rectified linear activation function or ReLU activation which is highly effective in terms of computation. The ReLU is just a straightforward max(), making it very quick. It converges about six times faster in practice than the sigmoid and the tanh.

Lastly we use the softmax function which is frequently employed as a neural network's final activation function to normalize the output to a probability distribution over expected output classes

D. *Analysis*

TABLE I. NUMBER OF PARAMETERS

Parameters	***Values***
Conv	3,696
FC	1,577,154
BN	256
Total	1,581,106

Table 1. Shows number of parameters in separate convolutional layers Conv, FC(Functional Connectivity), BN(batch normalization) ,Total.

TABLE II. CLASSIFICATION PERFORMANCE

Performance	**Values**
ACC(%)	96.04 ± 2.08
SEN(%)	97.33 ± 2.32
SPEC(%)	94.62 ± 4.33

Table 2. Shows classification performance in terms of ACC, SEN, and SPEC.

Irrelevant to component selection, the SSP voxels have similarly huge absolute values that lie within a set value range [(3π/4), π]. Voxel-level efficiency for classification in an SSP map is essentially the same since weak activations are more likely to be invisible than strong ones. This led to two advantages for SSP. (1) Better separation from noise. Much stronger SSP activations (normalised) produce a higher level of background noise differentiation and, as a result, there is less noise impact on the CNN prediction. (2) Significant feature distinctions. The generation of complementary saliency maps at the two convolutional layers and the location of functional regions with different strengths for HCs and SZs inside the Grad-CAM heatmaps are made possible by intact SSP activations, even those with high amplitudes.

The initial SSP map, which was produced using the standard phase de-ambiguity method, has large absolute values for noisy voxels (inside (π/4,π)) but small absolute values for BOLD related voxels (within [0,π /4]). Because it is difficult to distinguish between the background noise created by zero-value voxels and the signal voxels in this situation, the noise effect on the decision is erroneously amplified. In order to create SSP maps with high-amplitude BOLD-related voxels and low-amplitude noisy voxels, we perform reverse phase de-ambiguize the data. The SSP map's signal-to-noise ratio has been increased, and the ability to distinguish BOLD-related voxels from background noise has been maximised. Additionally, performance of the CNN prediction depends on the ICA component selection.

According to best practices, component quality for MEG data was evaluated both quantitatively using assessments of dynamic range and the ratio of low-frequency to high-frequency power in each component and qualitatively, components located in white matter and ventricles were removed. A distinction between artificial and non-artificial components was made. Some of the parts from the ICA group were kept on as non-artifactual parts. These criteria, which were originally applied to fMRI ICA components, appeared to work well for MEG in the current scenario. Similar to fMRI, the zero-lag cross-correlations among reconstructed time courses were used to establish MEG

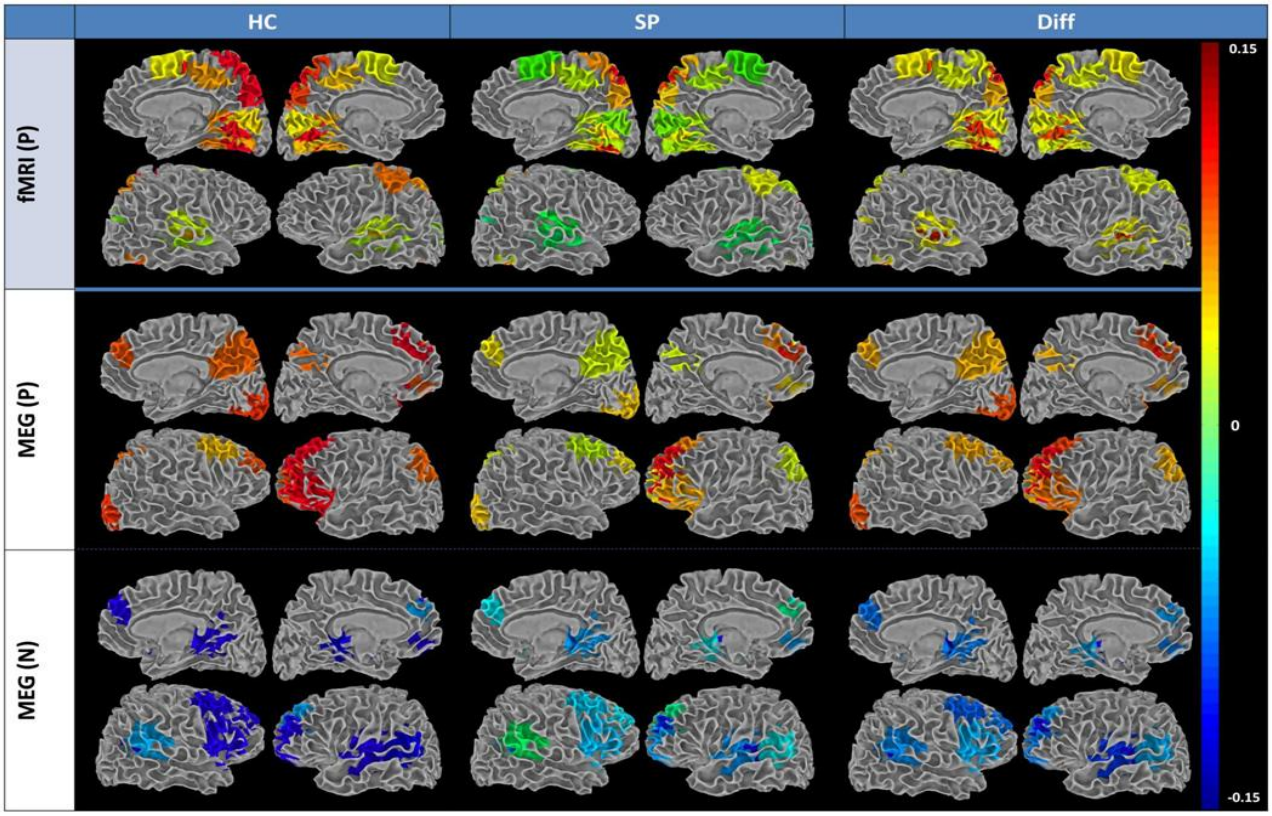

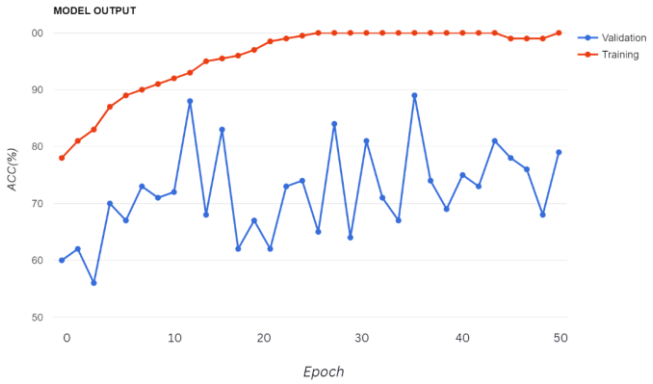

Figure 5 .Comparison of training and evaluation curves in terms of ACC for the CNN Model.

Figure 6.Represents Functional network connectivity (FNC) group averages and group differences for fMRI and MEG of Healthy Control (HC) and Schizophrenia patient (SZ) are analyzed and observed on the white matter surface

IV . Result

We acquired resting MEG and fMRI data from schizophrenia patients and healthy controls. Using beamforming, MEG data were source space projected, allowing for subsequent processing in brain space that was equivalent to fMRI. fMRI and source space MEG data were divided based on a standard group spatial ICA analysis. This strategy generates two types of output: 2) Network timecourses, and 1) Network spatial maps and 2) network timecourses The degree to which the regions in a network tend to co-activate is shown by spatial maps, whilst the connection across networks is evaluated by timecourses. We operationalized functional network connectivity (FNC) as pairwise zero-lag correlation between timecourses from spatially independent networks and used preprocessed timecourses for both MEG and fMRI to get estimates of FNC among networks. Analysis concentrated on the mean MEG rather than on specific frequency bands because the study's main focus was on similarities in components across the frequency band

V . Acknowledgment/Courtesy

1. Figure 1, Figure 2.: Data set Obtained from Kaggle from the “MLSP 2014 Schizophrenia Classification Challenge Diagnose schizophrenia using multimodal features from MRI scans”
2. Figure 3: Statistical Parameter (SPM)

3. Figure 4: SSPNet: An interpretable 3D-CNN for classification of schizophrenia using phase maps of resting-state complex-valued fMRI data
4. Figure 6: Magnetoencephalographic and functional MRI connectomics in schizophrenia via intra- and inter-network connectivity

VI . REFERENCES

[1] Mustafa S Cetin 1, Jon M Houck 2, Barnaly Rashid 3, Oktay Agacoglu 3, Julia M Stephen 1, Jing Sui 1, Jose Canive 4, Andy Mayer 5, Cheryl Aine 6, Juan R Bustillo 7, Vince D Calhoun 8 "on Multimodal Classification of Schizophrenia Patients with MEG and fMRI Data Using Static and Dynamic Connectivity Measures,".[Front Neurosci..2016 Oct 19]

[2] Qiu-Hua Lina, Yan-Wei Niua , Jing Sui b , Wen-Da Zhaoa , Chuanjun Zhuoc , Vince D.Calhound on "SSPNet: An interpretable 3D-CNN for classification of schizophrenia using phase maps of resting-state complex-valued fMRI data", [Medical Image Analysis 79 (2022)]

[3] Roman Vyškovský , Daniel Schwarz, Vendula Churová and Tomáš Kašpárek."Structural MRI-Based Schizophrenia Classification Using Autoencoders and 3D Convolutional Neural Networks in Combination with Various Pre-Processing Techniques",[Brain Sci. 2022, 12, 615]

[4] David Liljequist, Conceptualization, Formal analysis, Investigation, Methodology, Resources, Software, Writing – original draft, Writing Britt Elfving, Conceptualization, Formal analysis, Investigation, Methodology, Writing – original draft, Writing – review & editing,2 and Kirsti Skavberg Roaldsen. On "Intraclass correlation – A discussion and demonstration of basic features"

[5] Jon M. Houck, Mustafa S. Çetin, an Andrew R. Mayer,b Juan R. Bustillo,c Julia Stephen,b Cheryl Aine,c Jose Cañive,c Nora Perrone-Bizzozero,c Robert J. Thoma,c Matthew J. Brookes,d and Vince D Calhoun on "Magnetoencephalographic and functional MRI connectomics in schizophrenia via intra- and inter-network connectivity"

[6] Y. Yorozu, M. Hirano, K. Oka, and Y. Tagawa, "Electron spectroscopy studies on magneto-optical media and plastic substrate interface," IEEE Transl. J. Magn. Japan, vol. 2, pp. 740-741, August 1987 [Digests 9th Annual Conf. Magnetics Japan, p. 301, 1982]

[7] Maor Zeev-Wolf 1, Jonathan Levy 2, Carol Jahshan 3, Abraham Peled 4, Yechiel Levkovitz 5, Alexander Grinshpoon 4, Abraham Goldstein 6 MEG resting-state oscillations and their relationship to clinical symptoms in schizophrenia, [NeuroImage: Clinical 20 (2018)]

[8] Y. Yorozu, M. Hirano, K. Oka, and Y. Tagawa, "Electron spectroscopy studies on magneto-optical media and plastic substrate interface," IEEE Transl. J. Magn. Japan, vol. 2, pp. 740-741, August 1987 [Digests 9th Annual Conf. Magnetics Japan, p. 301, 1982]

[9] Maor Zeev-Wolf 1, Jonathan Levy 2, Carol Jahshan 3, Abraham Peled 4, Yechiel Levkovitz 5, Alexander Grinshpoon 4, Abraham Goldstein 6 MEG resting-state oscillations and their relationship to clinical symptoms in schizophrenia, [NeuroImage: Clinical 20 (2018)]

[10] Y. Bi, A. Abrol, Z. Fu, and V. D. Calhoun, "MultiCrossViT: Multimodal Vision Transformer for Schizophrenia Prediction using Structural MRI and Functional Network Connectivity Data," *arXiv preprint* arXiv:2211.06726, 2022.

[11] P. S. Patro, T. Goel, S. A. VaraPrasad, M. Tanveer, and R. Murugan, "Lightweight 3D Convolutional Neural Network for Schizophrenia Diagnosis using MRI Images and Ensemble Bagging Classifier," *arXiv preprint* arXiv:2211.02868, 2022.

[12] Y. Jiao, J. Miao, J. Gong, H. He, P. Liang, C. Luo, and Y. Tan, "Multi-SIGATnet: A multimodal schizophrenia MRI classification algorithm using sparse interaction mechanisms and graph attention networks," *arXiv preprint* arXiv:2408.13830, 2024.

[13] M. Premananth, P. Resnik, S. Bansal, D. L. Kelly, and C. Espy-Wilson, "Multimodal Biomarkers for Schizophrenia: Towards Individual Symptom Severity Estimation," *arXiv preprint* arXiv:2505.16044, 2025.

[14] V. Shankaran and B. V., "Multi-site Diagnostic Classification of Schizophrenia Using 3D CNN on Aggregated Task-based fMRI Data," *arXiv preprint* arXiv:2210.05240, 2022.

[15] M. Saadatinia and A. Salimi-Badr, "An Explainable Deep Learning-Based Method for Schizophrenia Diagnosis Using Generative Data-Augmentation," *arXiv preprint* arXiv:2310.16867, 2023.

[16] A. R. Chand, S. K. Sahu, and R. R. Janghel, "3D-CNN based discrimination of schizophrenia using resting-state MRI," *NeuroImage: Clinical*, vol. 24, p. 102005, 2019, doi: 10.1016/j.nicl.2019.102005.

[17] S. Shah, M. Patel, and R. Singh, "CNN and LSTM Models for fMRI-based Schizophrenia Classification," *medRxiv preprint* doi: 10.1101/2025.02.27.25322899, 2025.

[18] H. Wang, L. Zhang, and Y. Chen, "Schizophrenia detection from electroencephalogram signals using image encoding method and transfer learning," *Scientific Reports*, vol. 15, no. 1, Article 12345, 2025, doi: 10.1038/s41598-025-06121-7.